Electrostatics and Electrodynamics of Bacteriorhodopsin

Dietmar Porschke
Max Planck Institut für Biophysikalische Chemie, D-37077 Göttingen, Germany

ABSTRACT The stationary electric dichroism of bacteriorhodopsin is in qualitative, but not quantitative, agreement with the orientation function for disks having a permanent dipole directed perpendicular to the plane and an induced dipole in the plane. Fits of the orientation function to data measured at low field strengths demonstrate: an increase of the permanent dipole moment μ with the square of the disk radius r^2, whereas the polarizability α increases with r^4; the ionic strength dependence is small for μ and clearly stronger for α; the permanent dipole moment is 4×10^6 D at $r = 0.5$ μm. According to the risetime constants, the induced dipole does not saturate and increases to 4×10^8 D at 40 kV/cm and $r = 0.5$ μm. The data indicate that the permanent dipole is not of some interfacial character but is due to a real assymetry of the charge distribution. The experimental dipole moment per protein monomer is ~55 D, whereas calculations based on the structure of Grigorieff et al. (Grigorieff, N., T. A. Ceska, K. H. Downing, J. M. Baldwin, and R. Henderson. 1996. Electron-crystallographic refinement of the structure of bacteriorhodopsin. *J. Mol. Biol.* 259:393–421) provide a dipole moment of ~570 D. The difference is probably due to a nonsymmetric distribution of charged lipid residues. It is concluded that experimental dipole moments reflect the μ-potential at the plane of shear for rotational diffusion, in analogy to the ζ-potential used for translational diffusion. It is suggested that the permanent dipole of bacteriorhodopsin supports proton transport by attraction of protons inside and repulsion of protons outside of the cell. Dichroism rise curves at field strengths between $E = 150$ and 800 V/cm reveal an exponential component with time constants τ_3^r in the range between 1 and 40 ms, which is not found in Brownian dynamics simulations on a disk structure using hydrodynamic and electric parameters characteristic of bacteriorhodopsin disks. The experimental data suggest that this process reflects a cooperative change of the bacteriorhodopsin structure, which is induced already at a remarkably low field strength of ~150 V/cm.

INTRODUCTION

The electric parameters of bacteriorhodopsin have been studied in many different investigations by a large number of authors (Shinar et al., 1977; Keszthelyi, 1980; Druckmann and Ottolenghi, 1981; Kimura et al., 1981, 1984; Barabás et al., 1983; Kahn and Tu, 1984; Stoylov et al., 1984; Papp et al., 1986; Taneva et al., 1987, 1992). The analysis of electric parameters is closely related to that of field-induced reactions in bacteriorhodopsin, which have also been discussed extensively (Tsuji and Neumann, 1981a,b; 1983; Tsuji and Hess, 1986, 1990; Tsuji et al., 1988). In spite of this considerable activity, the views on the nature of the remarkable electric parameters of bacteriorhodopsin did not converge yet. Although there is experimental evidence indicating the existence of a high permanent electric dipole moment associated with bacteriorhodopsin, it has been suggested that at least part of the membrane charge asymmetry is of an interfacial or electrokinetic nature (e.g., Taneva et al., 1992). An unequivocal decision on the nature of electric parameters of macromolecules and of macromolecular complexes is not trivial at all, because there is a large number of different effects that may contribute to a given experimental phenomenon. Until now the assignment of dipole moments and of polarizabilities has been based on electrooptical measurements performed at different frequencies. Using this approach, several authors (Barabás et al., 1983; Kimura et al., 1984; Papp et al., 1986) concluded that the electrooptical data observed for standard bacteriorhodopsin preparations are consistent with a disk model having a permanent dipole perpendicular to its plane and a high polarizability parallel to this plane. The orientation function for this case has been developed many years ago by Shah (1963). However, Shah's orientation function has not been applied yet for any quantitative analysis of data over a sufficiently wide range of experimental conditions. This appears to be partly due to the mathematical complexity of this function. According to the literature, all applications presented until now remained limited to simple approximations, which can be valid only in a restricted range of conditions.

In the present investigation electrooptical data have been collected for a wide range of experimental conditions. By using a special pulse generator it has been possible to apply relatively long electric field pulses without any decay of the field strength E up to rather high E-values. Thus, stationary values of the electric dichroism could be measured over a wide range of electric field strengths and ionic strengths. The dichroism values obtained at different field strengths have been analyzed quantitatively according to the orientation function described by Shah (1963). The results provide more substantial evidence for the existence of a true permanent asymmetry of the charge distribution in bacteriorhodopsin, but also demonstrate clear deviations between experimental data and the standard model.

Received for publication 6 June 1996 and in final form 25 September 1996.
Address reprint requests to Dr. Dietmar Porschke, Max Planck Institut für Biophysikalische Chemie, Karl-Friederich-Bonhoffer Inst., Am Fassberg 11, D-37077 Göttingen, Germany. Tel.: 49-551-2011438; Fax: 49-551-2011435; E-mail: dpoersc@gwdg.de.

0006-3495/96/12/3381/11 $2.00

A detailed analysis of the electrooptical transients and a comparison with results of Brownian dynamics simulations demonstrates the existence of a special process, which does not reflect simple field-induced rotational relaxation of membrane disks. This process reveals information about the internal electrodynamics of bacteriorhodopsin disks.

MATERIALS AND METHODS

Bacteriorhodopsin samples were kindly provided from the laboratory of D. Oesterhelt. These samples were analyzed after extensive dialysis against the buffers used for the measurements. The standard buffer contained 1 mM NaCl, 1 mM sodium cacodylate pH 7.0, and 0.2 mM EDTA. The other buffers mentioned in the text were prepared either by dilution or by addition of NaCl. To suppress aggregation, the samples were sonicated before measurements; for this type of sonication a relatively weak source of ultrasound was used to avoid destruction of the membrane disks: the samples contained in a glass vessel were sonicated in the bath of a Bransonic 220 for 2 to 3 min. Part of the samples were subjected to strong sonication for preparation of smaller membrane fragments by a Branson sonifier B12. After sonication these samples were separated according to their size by gel filtration on Sepharose 4B (Pharmacia, Uppsala, Sweden) in 0.1 M NaCl, 1 mM sodium cacodylate pH 7.0, and 0.2 mM EDTA. The fractions were dialyzed into the standard buffer for the measurements. Usually the samples were analyzed at concentrations corresponding to an absorbance at 546 nm of 0.02 to 0.05 at a light path of 1 cm. Concentrations were calculated using an extinction coefficient of 63,000 $M^{-1}\,cm^{-1}$ at 568 nm (Oesterhelt and Hess, 1973). All the data reported below are for the light-adapted form of bacteriorhodopsin. All samples showed the absorbance maximum at 568 nm characteristic of the native form of bacteriorhodopsin. The size of our bacteriorhodopsin samples was determined from the dichroism decay time constants τ_d: using an equation for the rotational relaxation time constant τ_d of thin circular disks (Perrin, 1934), the diameter b of the disks was calculated according to

$$b = \sqrt[3]{\frac{9kT}{2\eta}\,\tau_d} \qquad (1)$$

where η is the viscosity of the medium and kT the thermal energy.

Electric field pulses in the low field regime were generated by a programmable arbitrary waveform generator AWG 5105 from Tektronix. The pulses were amplified by a precision power amplifier 5205A from Fluke. The samples were subjected to the electric field pulses in a standard cuvette with 1 cm optical pathlength with an insert machined from Teflon holding platinum electrodes at a distance of 4.8 mm. The linear dichroism signals were recorded by an optoelectronic detection system constructed for measurements of temperature jump relaxation: a 100 W halogen tungsten lamp was used as a light source together with a Schoeffel GM250 grating monochromator; the dichroism was measured at 546 nm using a Glan polarizer from calcite obtained from Halle (Berlin); part of the light beam was reflected by a quartz plate on a reference multiplier; the reference signal was used for compensation of fluctuations of the light intensity by a simple analog electronics device. The dichroism transients were recorded together with the electric field pulses by a Tektronix DSA602 digital signal analyzer. The data were transmitted to a PC, where a simple graphics routine was used for analysis of changes of stationary light intensities. Pulses of high electric field strength were generated by the cable technique: the setup used for pulse generation was a modified version of that described by Grünhagen (1974); the setup used for detection has been briefly described by Porschke (1980). Any influence of electrode polarization on the electric field strength in the samples has not been considered, because it should be negligible for the essential experimental data obtained in the present investigation. Dichroism transients were analyzed after transfer of the data to the facilities of the Gesellschaft für wissenschaftliche Datenverarbeitung mbH, Göttingen, by a set of programs developed for analysis of chemical and physical relaxation, including programs for deconvolution.

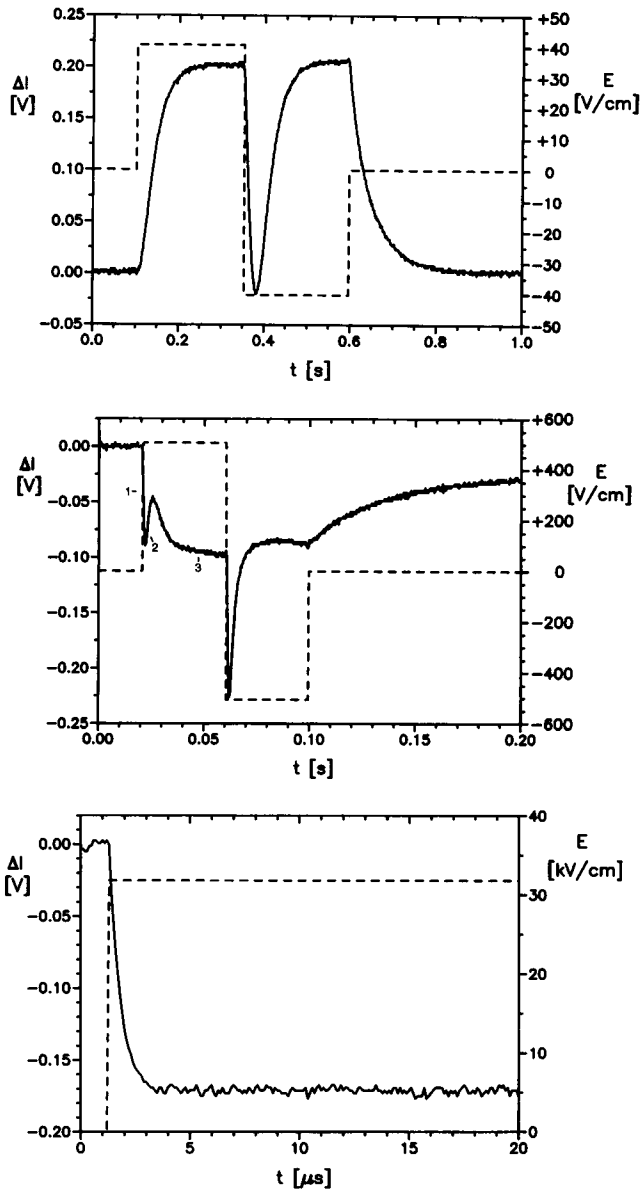

FIGURE 1 Change of the light intensity (ΔI) transmitted by a bacteriorhodopsin solution induced by pulses of different electric field strengths E. The light of wavelength 546 nm was polarized parallel to the field vector (standard buffer, 20°C). The transients shown in (*a*) and (*b*) were obtained by the pulse generator for low electric field strengths, whereas the transient (*c*) was obtained by the cable technique (without reversal of the field vector; cf. Materials and Methods). The exponential processes of the rise curve in (*b*) are indicated by 1, 2, and 3 (see Electrodynamics).

RESULTS

Electrostatics

The electric dichroism of bacteriorhodopsin is known to be very large and can be measured without problems. The data described below have been mainly measured with the plane

of polarization parallel to the field vector. Controls at the magic angle orientation did not indicate changes of the bacteriorhodopsin structure induced by the field pulses under the conditions of the present investigation. It should be noted that there may be field-induced conformation changes that are not indicated by absorbance changes under magic angle conditions (see Electrodynamics). As shown by the examples in Fig. 1, the electric field pulses were always sufficiently long to ensure complete adjustment of the stationary equilibrium of the orientation (transients are discussed in Electrodynamics). The stationary changes of the light intensity were used to calculate the stationary dichroism according to

$$\Delta\epsilon/\epsilon = \frac{\Delta A_{\parallel} - \Delta A_{\perp}}{\bar{A}} = \frac{1.5 \cdot \Delta A_{\parallel}}{\bar{A}} \tag{2}$$

where $\Delta A_{\parallel}$ and $\Delta A_{\perp}$ are the field-induced absorbance changes measured by light polarized parallel and perpendicular to the field vector, respectively; $\bar{A}$ is the absorbance in the absence of an external electric field. The dichroism is negative at low electric field strengths E and shows a minimum at relatively low E-values (Fig. 2); for samples of large size (radius $r = 0.5$ μm) the minimum appears at $E \sim 100$ V/cm and the dichroism changes its sign at $E \sim 500$ V/cm. This special dependence of the dichroism on the field strength is consistent with the orientation function for disks having a permanent dipole moment μ in perpendicular direction to their plane and a preferential polarizability α in the direction of the plane. This orientation function has been described by Shah (1963)

$$\Delta\epsilon/\epsilon = -2 \cdot \Phi \cdot (\Delta\epsilon/\epsilon)_{\infty} \tag{3a}$$

$$\Phi = \frac{3}{4\gamma} \tag{3b}$$

$$\left[\frac{\beta^2}{2\gamma} + 1 + \frac{e^{-((\beta^2/4\gamma)+\gamma)}\left[\frac{\beta}{\sqrt[2]{\gamma}}(e^{-\beta} - e^{\beta}) - \sqrt{\gamma}(e^{-\beta} + e^{\beta})\right]}{I}\right] - \frac{1}{2}$$

where

$$I = \int_{t1}^{t2} e^{-x^2} dx \tag{3c}$$

$$t1 = -\sqrt{\gamma} - \beta/2\sqrt{\gamma} \qquad t2 = \sqrt{\gamma} - \beta/2\sqrt{\gamma}$$

$$\beta = -\mu E/kT \tag{3d}$$

$$\gamma = -\alpha E^2/2kT \tag{3e}$$

$(\Delta\epsilon/\epsilon)_{\infty}$ is the value of the reduced dichroism in the limit of high electric field strengths, E the electric field strength, and kT the thermal energy.

The orientation function (Eq. 3) has been coded in Fortran and combined with an efficient least-squares fitting routine. Fitting of the experimental data shows that data measured over a range of electric field strengths up to 500 V/cm cannot be represented by the orientation function at a sufficient accuracy (cf. Fig. 2). The difference between theoretical expectation and experimental results may be due to different reasons. One of the potential reasons is a size heterogeneity of the samples. Thus, the size distribution was examined by a careful analysis of the dichroism decay curves. The decay curves obtained for the original samples, which have been subjected to a short treatment by ultrasound of relatively low energy in order to suppress aggregation, could be fitted by single exponentials at a high accuracy. Furthermore, the time constants τ^d evaluated from decay curves measured after pulses of widely different electric field strength remained within a narrow range, defined by the usual limits of experimental accuracy. It should be mentioned that dichroism decay time constants are very sensitive indicators of the size and, thus, any significant size variation should be easily detectable. According to these results the size distribution of the large bacteriorhodopsin disks used in our experiments was rather narrow.

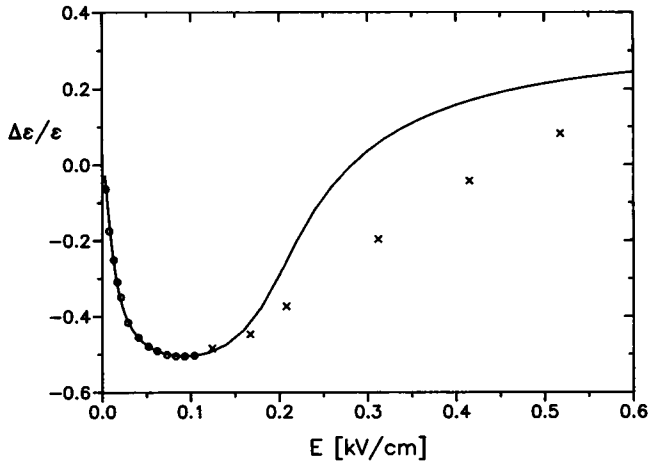

FIGURE 2 Reduced electric dichroism $\Delta\epsilon/\epsilon$ of bacteriorhodopsin as a function of the electric field strength E. The continuous line represents a least-squares fit of the data points (○) according to the orientation function (Eq. 3) with a permanent dipole moment $\mu = 1.19 \times 10^{-23}$ Cm, a polarizability $\alpha = 6.6 \times 10^{-28}$ Cm^2 V^{-1} and a limiting value of the dichroism $(\Delta\epsilon/\epsilon)_{\infty} = 0.31$; the experimental data marked by × were not included in the least-squares fit (standard buffer, 20°C).

The stationary values of the dichroism obtained for large bacteriorhodopsin disks with diameters in the range of 1 μm can be fitted by the orientation function, provided that the electric field strength remains limited to about 150 V/cm (cf. Fig. 2). The permanent dipole moment obtained from this fit is 1.19×10^{-23} Cm and the polarizability 6.6×10^{-28} Cm^2 V^{-1}. The permanent dipole moment corresponds to 3.6×10^6 D and the induced dipole moment at a field strength of 100 V/cm corresponds to 2×10^6 D. Both the permanent and the induced dipole moment are extremely high. This may suggest that the induced dipole moment is at the limit of its saturation and that the experimental dichroism at $E \geq 100$ V/cm lags behind the values extrapolated from the

dependence observed at lower field strengths, because the induced dipole does not increase with E as implied by Eq. 3.

The nature of the deviation has been studied in more detail by measurements of the dichroism response at high field strengths E. The stationary dichroism of bacteriorhodopsin disks increases with E in a range of E-values, where saturation of the orientation of the disks would be expected, if their electric parameters found at low field strengths would be valid up to high field strengths. The limit value of the dichroism approached at high field strengths in the range of 70 kV/cm is approximately 0.45. The limit dichroism of the same sample evaluated by least squares fitting of the dichroism measured at low field strengths to Eq. 3 is 0.34. It is difficult to get quantitative information from this gradual increase of the dichroism with E at high E-values. A more direct source of information are the time constants of rotation in the presence of the electric field. At low electric field strengths the rise of the dichroism is associated with more than a single time constant. At high field strengths (cf. Fig. 1 *c*), however, the rise curves can be fitted by single exponentials τ_i^r at a satisfactory accuracy. This is attributed to a much higher energy and thus also a much higher torque resulting from the induced dipole compared to that resulting from the permanent dipole at high field strengths. It is known that the reciprocal risetime $1/\tau_i^r$ of induced dipoles increases with E^2 at high E-values. As shown in Fig. 3, this relation is also found for bacteriorhodopsin disks in a wide range of field strengths. The slope $d(1/\tau_i^r)/d(E^2)$ observed in the range from 2 to 40 kV/cm is 2.2×10^{-7} m^2 s^{-1} V^{-2} and may be used to calculate the polarizability α according to an equation given by Schwarz (1956)

$$1/\tau_i^r = \frac{2 \cdot \alpha \cdot D_r}{kT \cdot x_0} E^2 \qquad (4)$$

where D_r is the coefficient for rotational diffusion and x_0 is a calibration factor. According to Schwarz the calibration factor is 3.35; recent numerical calculations (Antosiewicz et al., 1991) revealed a value of 2.9. Using the values x_0 = 2.90 and $D_r = 1/(6\,\tau^d) = 3.54\ s^{-1}$, the polarizability is α = 3.6×10^{-28} Cm^2 V^{-1}, which is surprisingly close to that derived from the stationary dichroism measured for the same sample (4.9×10^{-28} Cm^2 V^{-1}) at low field strengths by a least-squares fit to Eq. 3. This result indicates that the induced dipole does not saturate in the present case and is valid over a broad range of electric field strengths. The induced dipole of the sample used for the measurements shown in Fig. 3 increases to 4.3×10^8 D at 40 kV/cm.

More information on the nature of the electric parameters of bacteriorhodopsin was obtained from measurements on samples of various size. Samples of reduced size were prepared by sonication, followed by fractionation using gel filtration (see Materials and Methods). Depending on the energy of sonication and the duration of the treatment it was possible to prepare fragments of different sizes. However, in spite of the fractionation procedure, the samples prepared by this procedure were not as homogeneous as the original ones, as indicated by the dichroism decay curves, which required more than a single exponential for satisfactory fitting. The average size of the fragments was assigned according to the average dichroism decay time constants. The stationary values of the dichroism measured as a function of the electric field strength E arrived at the characteristic minimum at higher field strengths for samples of lower size. Least squares fitting of these data by the orientation function (Eq. 3) reveals a clear decrease of both the dipole moment μ and the polarizability α with decreasing size of the fragments. Linear regressions of $\log(\mu)$ and $\log(\alpha)$ versus $\log(\tau^d)$ provide the slopes 0.76 and 1.33, respectively (Fig. 4 and Fig. 5).

According to theory the dichroism decay time constant τ^d increases with the 3rd power of the disk radius (Eq. 1). If the

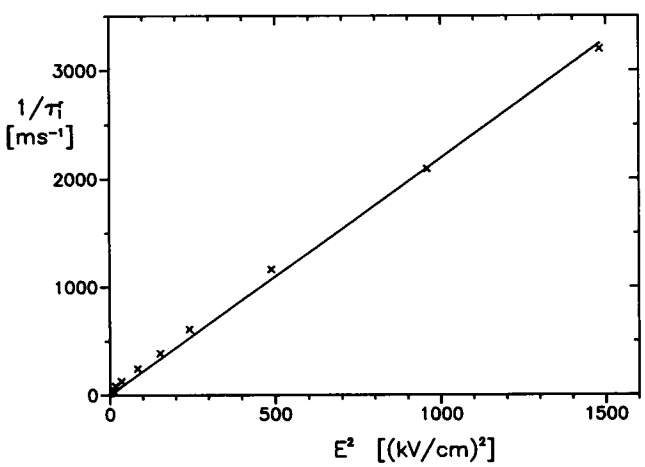

FIGURE 3 Reciprocal risetime $1/\tau_i^r$ of bacteriorhodopsin measured at "high" electric field strengths (see Fig. 1 *c*) as a function of the square of the electric field strength E^2. The straight line has been obtained by linear regression with intercept 0; the slope is 2.2×10^{-7} m^2 s^{-1} V^{-2} (standard buffer, 20°C).

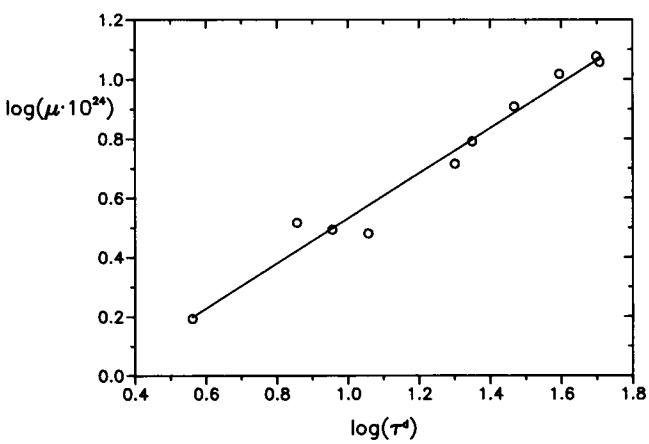

FIGURE 4 Logarithm of the permanent dipole $\log(\mu\times10^{24})$ of bacteriorhodopsin disks as a function of the logarithm of the dichroism decay time constant $\log(\tau^d)$. The straight line was obtained by linear regression; the slope is 0.76 (μ in units of Cm, τ^d in units of ms; standard buffer, 20°C).

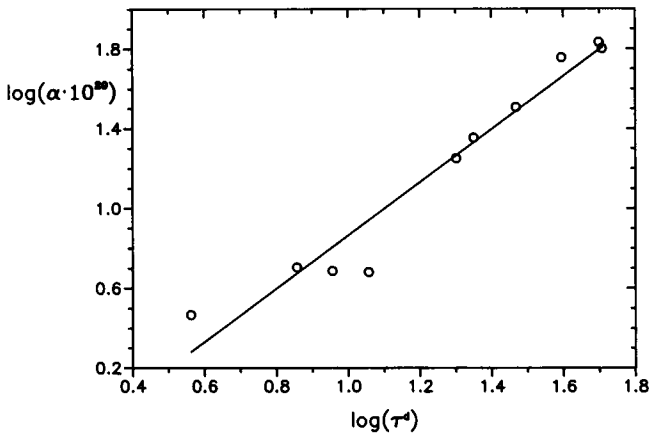

FIGURE 5 Logarithm of the polarizability $\log(\alpha \times 10^{29})$ of bacteriorhodopsin disks as a function of the logarithm of the dichroism decay time constant $\log(\tau^d)$. The straight line was obtained by linear regression; the slope is 1.33 (α in units of $Cm^2\ V^{-1}$, τ^d in units of ms; standard buffer, 20°C).

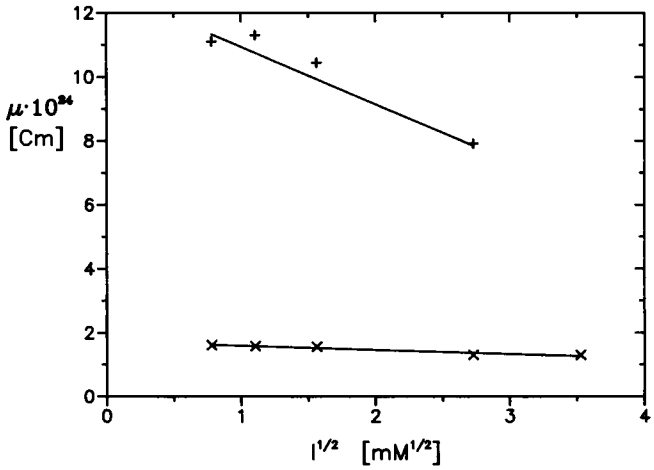

FIGURE 6 Permanent dipole moment μ of two bacteriorhodopsin samples of different size as a function of the square root of the ionic strength I. The data for a large size sample with $\tau^d = 67$ ms are indicated by + and for a small size sample with $\tau^d = 3.7$ ms by ×; the straight lines represent linear regressions with the slopes −1.8 and −0.13 for the larger and smaller samples, respectively.

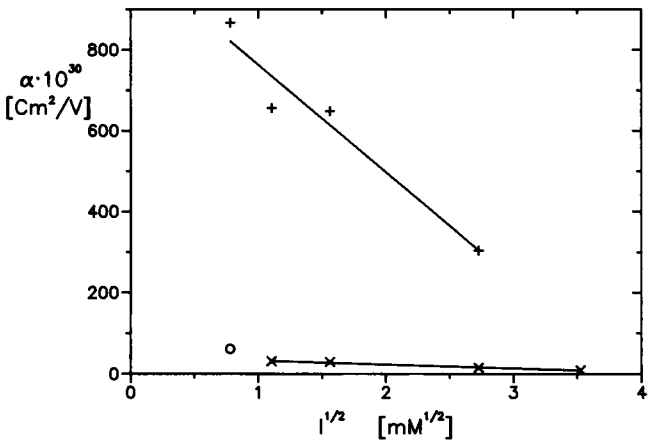

FIGURE 7 Polarizability α of two bacteriorhodopsin samples of different size as a function of the square root of the ionic strength I. The data for the larger samples with $\tau^d = 67$ ms are indicated by + and for the smaller sample with $\tau^d = 3.7$ ms by × (the measured value indicated by o was not included in the linear regression); the straight lines represent linear regressions with the slopes −265 and −9.6 for the larger and smaller samples, respectively.

dipole moment μ increases with the disk area, the slope expected from a linear regression of $\log(\mu)$ versus $\log(\tau^d)$ is 0.67. The observed slope is consistent with this expectation. Because the number of bacteriorhodopsin molecules increases linearly with the disk area, the observed dependence is consistent with a permanent anisotropy of the charge distribution in bacteriorhodopsin. The corresponding slope observed for the polarizability α is identical with that expected for an increase of α with the 4th power of the disk radius.

Another valuable indication for the nature of the electric parameters is their dependence on the salt concentration. For this reason the electric dichroism of bacteriorhodopsin samples has been measured at various ionic strengths and the resulting data were again analyzed in terms of the orientation function (Eq. 3). The permanent dipole moments μ obtained by this procedure show a relatively small decrease at an increase of the ionic strength I from 0.61 to 12.4 mM. The μ-values obtained for two bacteriorhodopsin samples of different size can be represented as a linear function of the square root of the ionic strength at a reasonable accuracy (Fig. 6). The slopes obtained for the two samples by linear regression are quite similar, if these values are given relative to the magnitude of the μ-values.

The polarizabilities derived from the same set of experimental data show a much higher dependence on the ionic strength (cf. Fig. 7). This dependence indicates that the polarizability reflects a property of the ion atmosphere around the bacteriorhodopsin disks.

Finally, the experimental data may be used to calculate the permanent dipole moment of a single bacteriorhodopsin molecule. Using a linear regression of the dipole moments obtained for samples of different size in the standard buffer against the disk area, together with the area of a single bacteriorhodopsin molecule of 11.5 nm^2 (Unwin and Henderson, 1975; Henderson et al., 1990), the molecular dipole moment is 55 *D*.

Model calculation

The structure of bacteriorhodopsin has been determined by electron cryo-microscopy up to a resolution of 3.5 Å in the direction of the membrane plane and of 4.3 Å perpendicular to this plane (Henderson et al., 1990; Grigorieff et al., 1996). In this structure "the positions of nearly all the important residues of bacteriorhodopsin are now well determined" (Grigorieff et al., 1996). The residues at both ends of the peptide chain, 1 to 6 and 228 to 248, are "genuinely disordered," but these residues must be close to the membrane surface and thus their contribution to the

dipole moment perpendicular to the membrane plane may be estimated at a reasonable degree of accuracy.

According to experimental and theoretical investigations of different proteins (Antosiewicz and Porschke, 1989a, 1995) it is known that the main contribution to dipole moments usually comes from the positive charges on arginine and lysine side chains and from the negative charges on aspartic and glutamic acid side chains. It is rather simple to calculate the dipole moment resulting from these residues in the protein core according to the model. Using the coordinates 2brd of the Brookhaven Protein Data Bank, the calculation shows that the dipole component perpendicular to the membrane plane is 145 *D*; the other orthogonal components are 303 and 32 *D*. However, these dipole components do not include the contribution from the terminal residues yet.

For a reasonable estimate of their contribution to the dipole moment perpendicular to the membrane plane, it should be sufficient to count the number of charges of the terminal residues "inside" and "outside" and multiply this number with the membrane thickness. A minor complication results from the fact that there are five negative charges inside and no charges outside. Because the dipole moment is defined by the torque, the five negative charges on the inside are considered with a lever of half of the membrane thickness. Using a membrane thickness of 6 nm, the dipole component from the terminal residues is 719 *D* directed from the inside to the outside. The sum of the core and the loop residues is 574 *D* in the direction from inside to outside. Obviously, this dipole moment should be regarded as approximate. It should be mentioned that the dipoles of the α-helices hardly contribute, because most of their dipole components compensate each other and thus the combined contribution resulting from the α-helices is negligible compared to that resulting from residues bearing full charges.

Electrodynamics

The electrooptical data in Fig. 1 demonstrate the existence of three different types of dichroism rise curves (observed during application of the first pulse): 1) the dichroism rise curves found in the low field regime require two exponentials for a satisfactory representation; in this regime all the observations are consistent with the existence of a permanent dipole; 2) at high field strengths the dichroism rise can be described by a single exponential at a satisfactory accuracy; all the observations in this range, including the field strength dependence of the rise time constant, are consistent with the dominant contribution from an induced dipole; 3) in an intermediate range of electric field strengths the dichroism rise curves clearly show the existence of three relaxation processes (cf. Fig. 1 *b*); the assignment of these processes requires a detailed analysis.

According to theory, electrooptical transients may involve up to eight relaxation times during rise and reversal (Wegener, 1986), with only five of these present during decay (Wegener et al., 1979). Analytical solutions for electrooptical transients have been presented only for simple limit cases. Transients for complex combinations of electrical parameters and also for the case of intermediate electric field strengths cannot be easily predicted, but may be generated by numerical simulations. For an assignment of the present experimental observations, electrooptical transients have been generated by Brownian dynamics simulations on a model using all the known parameters of bacteriorhodopsin disks.

According to all available informations standard bacteriorhodopsin samples are very well ordered in thin disk structures. For a simulation of the hydrodynamic parameters of such thin disks, the disk structure is represented by an assembly of beads as shown in Fig. 8. The beads are arranged in a hexagonal packing order to a circular disk with an effective diameter of 980 nm. The principal components of the diffusion tensor have been calculated by bead model simulations (Garcia de la Torre and Bloomfield, 1981; Antosiewicz and Porschke, 1989b). The resulting parameters have been used for the calculation of electrooptical transients using a Brownian dynamics simulation procedure described by Antosiewicz et al. (1991). Examples of electrooptical transients simulated for the different regimes of electric field strengths are given in Fig. 9.

A comparison of the calculated transients with the experimental ones demonstrates that there is a close agreement for the low- and the high-field regime. It should be noted that the experimental data shown in Fig. 1 represent changes of the transmitted light intensity, whereas the simulated data shown in Fig. 6 are given as changes of the dichroism: this is the reason for the opposite direction of the optical effects. A clear difference is found at intermediate electric field strengths, where the simulated dichroism rise curves show two main exponential components, whereas the experimental rise curves reveal three components. The difference demonstrates that the third component cannot be assigned to

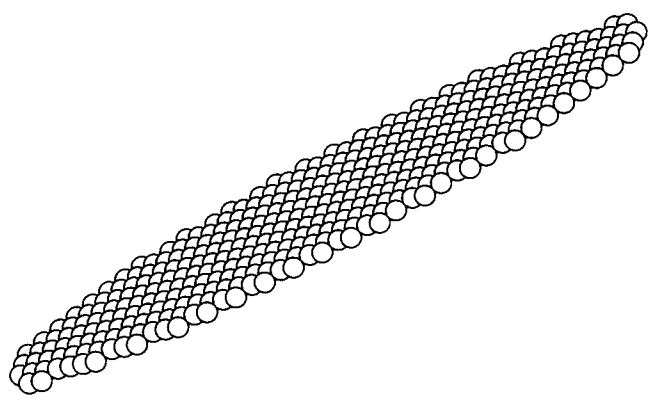

FIGURE 8 Bead model of a bacteriorhodopsin disk. 399 beads are arranged in hexagonal order in a circular disk. The effective diameter of the disk is 980 nm, the radius of individual beads is 14 nm. The bead model simulation provides the following principal components of the rotational diffusion tensor 3.081, 3.437, 3.411 (s^{-1}).

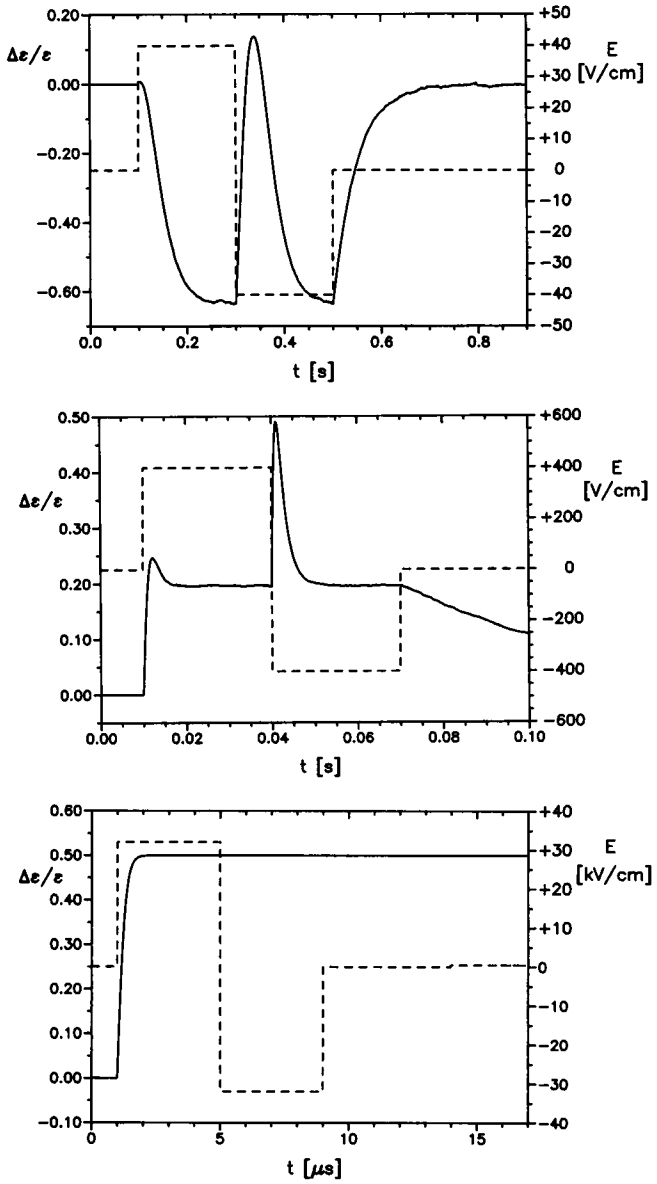

FIGURE 9 Brownian dynamics simulation of electrooptical transients of the disk shown in Fig. 8 using the following parameters: permanent dipole moment perpendicular to the plane 8.7×10^{-24} Cm, polarizability parallel to the plane 4.9×10^{-28} Cm^2 V^{-1}; extinction tensor: in plane components 76,000, component perpendicular to the plane 19,000. The transients *a-c* show the electric dichroism $\Delta\epsilon/\epsilon$ as a function of the time t in the different regimes of the electric field strength E.

a standard electrooptical response of a disk structure under the given conditions.

The transients given in Fig. 9 were calculated on the basis of a simple standard polarizability: it was assumed that the time constant for the induction of the induced dipole is small compared to the time scale of rotational diffusion. The experimental data demonstrate that there is indeed an induced dipole in bacteriorhodopsin with a small induction time constant. This does not exclude, however, that there is an additional induced dipole component with a large induction time constant in the ms time range. Thus, it is possible that the additional component observed for bacteriorhodopsin disks represents a slow polarization process. However, it is also possible that the additional component represents some field-induced change of the bacteriorhodopsin structure. As a basis for an assignment, some further information on the third process is required.

The additional process has been observed for given bacteriorhodopsin samples only in a rather limited range of electric field strengths, but in this range its time constant τ_3^r changes by an order of magnitude. τ_3^r can be represented as a linear function of the reciprocal electric field strength $1/E$ (Fig. 10). The high slope indicates that the reaction reflected by this relaxation process involves the cooperative response of many protein molecules—probably of the whole disk. The magnitude of the "cooperative size" may be studied by an analysis of the process in samples of different sizes. When the size of the bacteriorhodopsin disks is decreased, the additional process appears at higher electric field strengths. The time constants observed for different fragment sizes at various electric field strengths are compiled in Fig. 11 as a function of the reciprocal electric field strength. The data suggest that all the time constants τ_3^r can be represented by a general function, but it should be useful to analyze this feature in more detail in future.

Measurements over a range of different concentrations from 0.38 to 5.4 μM bacteriorhodopsin demonstrate that τ_3^r at fixed field strengths is independent of the concentration, within the limits of experimental accuracy. Thus, the additional process cannot be attributed to some *inter*molecular interaction, but reflects an *intra*molecular reaction.

It would be useful to characterize the transition range from the intermediate regime with three exponentials in the rise process to the high-field regime, where the rise curves can be represented by single exponentials. For technical

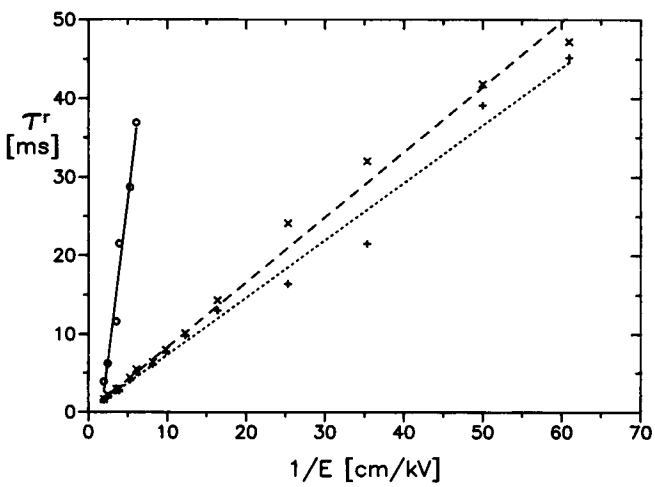

FIGURE 10 Dichroism rise time constants τ_1^r (+), τ_2^r (×), and τ_3^r (○) as a function of the reciprocal electric field strength $1/E$ (standard buffer, 20°C, the dichroism decay time constant of the bacteriorhodopsin sample is 47 ms). The straight lines represent linear regressions with the following slopes: τ_1^r 0.731 (· · ·); τ_2^r 0.828 (- - -); τ_3^r 8.14 (——), with intercept −13.5 (intercept = 0 in regressions for τ_1^r and τ_2^r).

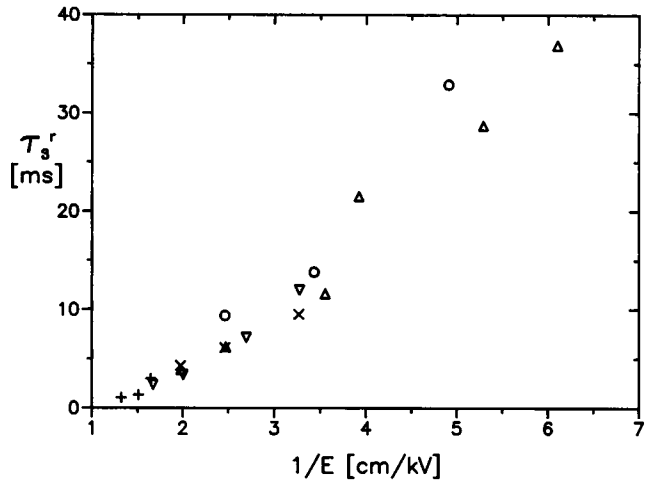

FIGURE 11 Dichroism risetime constant τ_3^r as a function of the reciprocal electric field strength $1/E$ for bacteriorhodopsin samples of different size. The dichroism decay time constants and the disk diameters derived from these values are: 51 ms–975 nm (×), 49.4 ms–965 nm (○), 47.1 ms–949 nm (△), 29.4 ms–811 nm (▽), 20 ms–714 nm (+).

reasons this range has not be analyzed yet in sufficient detail. Thus some problems associated with the additional process remain for further investigation.

DISCUSSION

Electrostatics

The electric parameters of bacteriorhodopsin are of special interest, partly because of the unusual magnitude of the permanent dipole moment and also because of a potential biological function of this dipole. The large permanent dipole moments observed for bacteriorhodopsin samples raised considerable doubts, whether these dipoles are due to a real permanent anisotropy of the charge distribution. The doubts partly result from the fact that dipole moments in the order of magnitude around 10^6 D are hard to imagine on the molecular level and partly from the observation of saturated, induced dipoles in linear polyelectrolytes like DNA double helices (cf. Diekmann et al., 1982). Thus, the interpretation of the electric parameters by interfacial or electrokinetic effects has been favored, e.g., by Taneva et al. (1992), and certainly it is not simple to falsify this view.

One of the reasons for another investigation of this subject is the fact that the appropriate orientation function has not been used for a quantitative analysis of electrooptical data yet. Previous investigations with assignments of dipole moments and polarizabilities were based on measurements at different frequencies, which involves some risk for the introduction of errors. For example, there may be a slow polarizability component that is not included by measurements at a frequency of a few kHz. The procedure used in the present investigation is more straightforward. Moreover, the concentrations used in the present investigation were an order of magnitude lower than those used for previous measurements. Under these conditions any artifacts resulting from field-induced interactions between bacteriorhodopsin disks have been avoided (cf. Porschke, 1985). Contributions from field-induced interactions were apparent under the conditions of previous measurements (cf. Barabás et al., 1983) and lead to particularly large perturbations under light scattering detection, but also affect measurements of the dichroism by changes of the turbidity.

The observed linear increase of the permanent dipole moment with the area of the membrane fragments supports the assignment of this dipole moment to a real asymmetry of the charge distribution. This assignment is also supported by the quite different dependence of the polarizability, which increases with the 4th power of the radius, corresponding to the square of the area. Furthermore, evidence for the existence of a true permanent dipole moment comes from the relatively small dependence of the permanent dipole on the ionic strength compared to the much higher ionic strength dependence of the polarizability.

Among the previous electrooptical investigations, the most detailed one has been reported by Kimura et al. (1984). These authors have used AC pulses for the characterization of the polarizability and found in their double logarithmic plot of the permanent dipole moment against the dichroism decay time constant a slope of 0.67, and in the corresponding plot for the polarizability a slope of about 1. Thus their conclusions on the size dependence are similar. However, the magnitudes of the parameters are different. The permanent dipole moment of Kimura et al. is higher than that found in the present investigation by a factor of approximately 2. The difference may be partly due to the experimental conditions (Kimura et al. measured at 4°C in 1 mM NaCl), but it is likely that the main difference results from the different procedures used for measurements and evaluation.

Apparently it has not been attempted yet to calculate the dipole moment of bacteriorhodopsin from its structure. Although the calculation can only be approximate, because part of the structure is disordered (Grigorieff et al., 1996), it provides clear evidence for the existence of a permanent dipole component in the direction perpendicular to the membrane plane. Obviously the existence of an asymmetry in the charge distribution in a single bacteriorhodopsin molecule adds up to huge dipole moments for membrane disks containing large numbers of these molecules in a well-ordered arrangement. The conceptional difficulty associated with these large dipole moments mainly results from the danger that these are misinterpreted in terms of point dipoles. Obviously the permanent dipole of bacteriorhodopsin disks is not a point dipole, but a multipole of unusual dimensions, which leads to a huge torque already at low field strengths.

One of the effects that must be associated with huge permanent dipole moments is electrostatic shielding by counterions. From this point of view, it may be surprising that external electrostatic fields induce a torque in the presence of an excess of counterions. The apparent problem is

analogous to that of charged lipid vesicles, which show electrophoretic motion although the charges are compensated at some distance from the surface. The electrophoretic motion of these particles is determined by the electrostatic potential at the plane of shear between the vesicle-associated and the stationary part of the double layer. This potential is called the ζ-potential (Helmholtz, 1879; Overbeek and Wiersema, 1967; McLaughlin, 1977). The ζ-potential has been defined for translational motion. In direct analogy, an effective dipole potential has to be defined, the "μ-potential," which determines the torque at the plane of shear for rotational diffusion. For the case of the ζ-potential it has been estimated that the thickness of the layer moving with the vesicles is about 0.2 nm. It is likely that the thickness of the corresponding layer in the case of the μ-potential is of very similar magnitude. This interpretation explains at least qualitatively that dipoles of proteins show a relatively weak dependence on the ionic strength, not only in the case of bacteriorhodopsin, but also in all the various cases that have been analyzed previously: lac-repressor (Porschke, 1987), α-chymotrypsin (Antosiewicz and Porschke, 1989a; Schönknecht and Porschke, 1996), acetylcholinesterase (Porschke et al., 1996).

According to the model calculation the permanent dipole of bacteriorhodopsin is directed from the inside of the cell to the outside. Some evidence supporting this assignment of the dipole direction comes from an experiment of Kimura et al. (1984): digestion by trypsin led to a reduction of the dipole moment determined by their procedure. According to Kimura et al. (1984) trypsin removed "one negative charge from the cytoplasmic side" and thus the electrooptical result is consistent with an in→out direction of the dipole. It should be possible now to use site-directed mutagenesis (cf. Mostafa et al., 1996; Hsu et al., 1996) to modify both magnitude and direction of the dipole moment and to compare theoretical expectations with experimental results. One of the problems remaining in the quantitative assignment of the electrostatic parameters is the contribution of lipids (cf. Jonas et al., 1990). It is very likely that the difference between the experimental and the calculated dipole moment mainly results from an asymmetry in the distribution of charged lipid residues.

Finally, the question should be discussed whether the permanent dipole contributes to the function of bacteriorhodopsin. The function is pumping of protons from the cell interior to the external medium driven by light absorption (cf. Stoeckenius et al., 1979; Lanyi, 1993). This function requires supply of protons to the pump entrance at the cytoplasmic side and removal of protons at the exit of the pump. Obviously both supply and removal of protons are based on diffusion. The efficiency of both processes may be increased by electrostatic potential gradients. At the entrance protons may be attracted by some negative potential, which may contribute via long-range electrostatic interactions to a considerable increase of the target size. At the exit protons may be pushed away by some positive potential. The combined negative entrance potential and the positive exit potential are equivalent with a permanent dipole moment. The direction of this dipole moment is consistent with the dipole calculated according to the molecular model of bacteriorhodopsin. Further investigations may demonstrate whether the large permanent dipole moments observed for other membrane proteins, e.g., Na^+/K^+-ATPase (Porschke and Grell, 1995), are also consistent with this interpretation.

Electrodynamics

Field-induced changes of the structure of membrane proteins are of considerable interest for processing bioelectricity. Evidence for field-induced conformation changes of bacteriorhodopsin from electrooptical measurements in solution has already been reported by Tsuji and Neumann (1981a, 1983). In a subsequent investigation Stoylov et al. (1984) analyzed the electrooptics of bacteriorhodopsin again and did not find "firm" evidence for a field-induced conformation change. An essential argument used by Tsuji and Neumann in their assignment of field-induced conformation changes is in contradiction with the results of the present investigation. Tsuji and Neumann (1981a, 1983) concluded that bacteriorhodopsin disks remain randomly distributed during short pulses of high electric fields and that the polarizability required for orientation of disks under these conditions is unrealistically high. The quantitative analysis presented above demonstrates that orientation of bacteriorhodopsin disks must be expected under the experimental conditions of Tsuji and Neumann.

The difficulty in the assignment of experimental observations results from the complexity of the system. Due to the presence of a permanent and an induced dipole moment in different directions, the field-induced orientation of bacteriorhodopsin disks is already a rather complex process. Furthermore, electric fields may induce some special effects, such as field-induced interactions, and thus it is not trivial to separate the different phenomena and to get unequivocal evidence for field-induced changes of conformations. In the present investigation the field-induced orientation of bacteriorhodopsin has been analyzed over a much broader range of field strengths than before and the data have been analyzed in more quantitative detail than previously. One of the results of this analysis is the detection of a "special" process, which has not been described before and does not fit into the standard scheme of orientation.

One of the possibilities for the assignment of the special process is a slow polarization reaction in the plane of the bacteriorhodopsin disks. It should be useful to compare the present data with results on the polarization of the counterion distribution around colloidal particles. According to experimental data obtained by Schwan et al. (1962) and a theoretical treatment by Schwarz (1962, 1972), the polarization time constant of spherical particles is given by

$$\tau_p = \frac{r^2}{2 \cdot D} \tag{5}$$

where r is the radius of the sphere and D is the surface diffusion coefficient of the counterions. For particles with a diameter of 1.17 μ a characteristic frequency of 480 Hz corresponding to a time constant of 300 μs was found by dielectric measurements, using low electric field strengths. The shape of the bacteriorhodopsin particles is not spherical, but counterion polarization of disks is expected to follow corresponding principles and thus is expected to occur in the same time range with a similar dependence on the size. The time constant of the special process observed for bacteriorhodopsin disks of 1 μm diameter is about 40 ms at low electric field strengths. This magnitude suggests that the special process does not reflect a standard polarization reaction with a shift of ions along the disk plane. For such a polarization process a strong dependence of its time constant on the size of the disks should be expected. The evidence for a function describing the time constants observed at different field strengths including data obtained for different disk sizes (cf. Fig. 11) is hardly consistent with an assignment to a standard polarization of the counterion distribution.

The most direct argument for a field-induced conformation change would be the observation of field-induced absorbance changes under magic angle conditions. In the present investigation some effects at the magic angle have been observed, but these effects are not considered to be sufficiently large as a proof for the existence of field-induced conformation changes. However, field-induced conformation changes are not necessarily reflected by absorbance changes of sufficient magnitude for experimental analysis, but may be reflected more clearly by changes of the optical anisotropy.

The special effect is associated with an increase of the dichroism. A comparison of the limit dichroism obtained by analysis of the data measured at low field strengths according to Eq. 3 with the dichroism measured at high field strengths indicates that there is a change of the structure associated with an increase of the dichroism. Thus, the most direct and straightforward interpretation of the combined stationary and transient electrooptical data is in terms of a field-induced change of the bacteriorhodopsin structure. According to this interpretation, the special effect directly reflects this change of structure. The observed values of the dichroism indicate that the field-induced reaction leads to a change of the structure, which is equivalent to an average rotation of the chromophor from ~64° to ~69° with respect to the direction of the permanent dipole vector, or ~26° to ~21° with respect to the membrane plane. The results reported previously on the angular orientation of the retinal chromophor of bacteriorhodopsin are in the same range (Heyn et al., 1977; Barabás et al., 1983; Kimura et al., 1984; Earnest et al., 1986; Papp et al., 1986; Lin and Mathies, 1989).

Any field-induced transition of the conformation requires some change of the electric parameters associated with the transition. In the present case the transition is already observed at a remarkably low electric field strength in the range of 150 V/cm. The observed dependence of the time constant τ_3^r is hardly consistent with a quadratic dependence on the electric field strength, which would be expected for a field-induced transition driven by an increase of a polarizability. The alternative mechanism based on a change of a permanent dipole moment $\Delta\mu$ requires a $\Delta\mu$-value in the range of 1×10^{-24} Cm for the case of large bacteriorhodopsin disks. Although this may appear to be an unrealistically high order of magnitude, it is about 10% of the magnitude of the total dipole moment associated with large bacteriorhodopsin disks and thus seems to be reasonable, provided that the transition is a cooperative process of the whole membrane disk.

The results of the present investigation raise some problems that remain for further investigation. A major problem is the nature of the field-induced transition of the bacteriorhodopsin disks. Furthermore, it remains to be shown whether the field-induced transition is of biological relevance. The transition may be the feedback element required for explanation of oscillation phenomena recently found in liposomes containing bacteriorhodopsin (Tributsch and Bogomolni, 1994; Birge, 1994). It is remarkable that the transition in bacteriorhodopsin is induced already at a rather low electric field strength. Thus, bacteriorhodopsin disks are of great interest as a model for the analysis of bioelectric phenomena at low field strengths.

The expert technical assistance of Hartmut Dangendorf is gratefully acknowledged. The author is also indebted to Dr. Manfred Stockburger for discussions and for comments on the manuscript.

The facilities of the Gesellschaft für wissenschaftliche Datenverarbeitung mbH, Göttingen, were used for data evaluation.

REFERENCES

Antosiewicz, J., T. Grycuk, and D. Porschke. 1991. Brownian dynamics simulation of electrooptical transients for solutions of rigid macromolecules. *J. Chem. Phys.* 95:1354–1360.

Antosiewicz, J., and D. Porschke. 1989a. The nature of dipole moments: experimental and calculated permanent dipole of α-chymotrypsin. *Biochemistry.* 28:10072–10078.

Antosiewicz, J., and D. Porschke. 1989b. Volume correction for bead model simulations of rotational friction coefficients of macromolecules. *J. Phys. Chem.* 93:5301–5305.

Antosiewicz, J., and D. Porschke. 1995. Electrostatics of hemoglobins from measurements of the electric dichroism and computer simulations. *Biophys. J.* 68:655–664.

Barabás, K., A. Dér, Z. Dancsházy, P. Ormos, L. Keszthelyi, and M. Marden. 1983. Electro-optical measurements on aqueous suspension of purple membrane from halobacterium halobium. *Biophys. J.* 43:5–11.

Birge, R. R. 1994. Bacteriorhodopsin. A nonlinear proton pump. *Nature.* 371:659–660.

Diekmann, S., W. Hillen, M. Jung, R. D. Wells, and D. Porschke. 1982. Electric properties and structure of DNA restriction fragments from measurements of the electric dichroism. *Biophys. Chem.* 15:157–167.

Druckmann, S., and M. Ottolenghi. 1981. Electric dichroism in the purple membrane of halobacterium halobium. *Biophys. J.* 33:263–268.

Earnest, T. N., P. Roepe, M. S. Braiman, J. Gillespie, and K. J. Rothschild. 1986. Orientation of the bacteriorhodopsin chromophore probed by polarized Fourier transform infrared spectroscopy. *Biochemistry.* 25: 7793–7798.

Garcia de la Torre, J., and V. A. Bloomfield. 1981. Hydrodynamic properties of complex, rigid, biological macromolecules: theory and applications. *Q. Rev. Biophys.* 14:81–139.

Grigorieff, N., T. A. Ceska, K. H. Downing, J. M. Baldwin, and R. Henderson. 1996. Electron-crystallographic refinement of the structure of bacteriorhodopsin. *J. Mol. Biol.* 259:393–421.

Grünhagen, H. H. 1974. Entwicklung einer E-Feldsprungapparatur mit optischer Detektion und ihre Anwendung auf die Assoziation amphiphiler Elektrolyte. Ph.D. Thesis. Universität Braunschweig.

Helmholtz, H. 1879. Studien über electrische Grenzschichten. *Ann. Physik.* 7:337–382.

Henderson, R., J. M. Baldwin, T. A. Ceska, F. Zemlin, E. Beckmann, and K. H. Downing. 1990. Model for the structure of bacteriorhodopsin based on high-resolution electron cryo-microscopy. *J. Mol. Biol.* 213: 899–929.

Heyn, M. P., R. J. Cherry, and U. Müller. 1977. Transient and linear dichroism studies on bacteriorhodopsin: determination of the orientation of the 568 nm all-trans retinal chromophor. *J. Mol. Biol.* 117:607–620.

Hsu, K. C., G. W. Rayfield, and R. Needleman. 1996. Reversal of the surface charge asymmetry in purple membrane due to single amino acid substitutions. *Biophys. J.* 70:2358–2365.

Jonas, R., Y. Koutalos, and T. G. Ebrey. 1990. Purple membrane: surface charge density and the multiple effect of pH and cations. *Photochem. Photobiol.* 52:1163–1177.

Kahn, L. D., and S. Tu. 1984. Electric birefringence study of the purple membrane of halobacterium halobium. *Biopolymers.* 23:707–718.

Keszthelyi, L. 1980. Orientation of membrane fragments by electric field. *Biochim. Biophys. Acta.* 598:429–436.

Kimura, Y., M. Fujiwara, and A. Ikegami. 1984. Anisotropic electric properties of purple membrane and their change during the photoreaction cycle. *Biophys. J.* 45:615–625.

Kimura, Y., A. Ikegami, K. Ohno, S. Saigo, and Y. Takeuchi. 1981. Electric dichroism of purple membrane suspensions. *Photochem. Photobiol.* 33:435–439.

Lanyi, J. K. 1993. Proton translocation mechanism and energetics in the light-driven pump bacteriorhodopsin. *Biochim. Biophys. Acta.* 1183: 241–261.

Lin, S. W., and R. A. Mathies. 1989. Orientation of the protonated retinal Schiff base group in bacteriorhodopsin from absorption linear dichroism. *Biophys. J.* 56:653–660.

McLaughlin, S. 1977. Electrostatic potentials at membrane-solution interfaces. *In* Current Topics in Membranes and Transport. Vol. 7. F. Bronner and A. Kleinzeller, editors. Academic Press, New York. 71–144.

Mostafa, H. I. A., G. Váró, R. Tóth-Boconádi, A. Dér, and L. Keszthelyi, 1996. Electrooptical measurements on purple membrane containing bacteriorhodopsin mutants. *Biophys. J.* 70:468–472.

Oesterhelt, D., and B. Hess. 1973. Reversible photolysis of the purple complex in the purple membrane of *Halobacterium halobium*. *Eur. J. Biochem.* 37:316–326.

Overbeek, J. T., and P. H. Wiersema. 1967. The interpretation of electrophoretic mobilities. *In* Electrophoresis—Theory, Methods and applications. M. Bier, editor. Academic Press, New York. 1–52.

Papp, E., G. Fricsovszky, and G. Meszena. 1986. Electrodichroism of purple membrane. Ionic strength dependence. *Biophys. J.* 49: 1089–1100.

Perrin, F. 1934. Mouvement brownien d'un ellipsoide. Dispersion diélectrique pour des molécules ellipsoidales. *J. Physique.* 5:497–511.

Porschke, D. 1980. Structure and dynamics of a tryptophanpeptide-polynucleotide complex. *Nucleic Acids Res.* 8:1591–1612.

Porschke, D. 1985. Field induced interactions of phospholipid vesicles. *Biochemistry.* 24:7981–7986.

Porschke, D. 1987. Electric, optical and hydrodynamic parameters of lac repressor from measurements of the electric dichroism—High permanent dipole moment associated with the protein. *Biophysic. Chem.* 28: 137–147.

Porschke, D., C. Créminon, X. Cousin, C. Bon, J. Sussman, and I. Silman. 1996. Electrooptical measurements demonstrate a large permanent dipole moment associated with acetylcholinesterase. *Biophys. J.* 70: 1603–1608.

Porschke, D., and E. Grell. 1995. Electric parameters of Na^+/K^+-ATPase by measurements of the fluorescence-detected electric dichroism. *Biochim. Biophys. Acta.* 1231:181–188.

Schönknecht, T., and D. Porschke. 1996. Electrooptical analysis of α-chymotrypsin at physiological salt concentration. *Biophys. Chem.* 58:21–28.

Schwan, H. P., G. Schwarz, J. Maczuk, and H. Pauly. 1962. On the low frequency dielectric dispersion of colloidal particles in electrolyte solution. *J. Phys. Chem.* 66:2626–2635.

Schwarz, G. 1956. Zur Theorie der Leitfähigkeitsanisotropie von Polyelectrolyten in Lösung. *Z. Physik.* 145:563–584.

Schwarz, G. 1962. A theory of the low frequency dielectric dispersion of colloidal particles in electrolyte solution. *J. Phys. Chem.* 66:2636–2642.

Schwarz, G. 1972. Dielectric polarization phenomena in biomolecular systems. *In* Dielectric and Related Molecular Processes, Vol. 1. The Chemical Society, London.

Shah, M. J. 1963. Electric birefringence of bentonite. II. An extension of saturation birefringence theory. *J. Phys. Chem.* 67:2215–2219.

Shinar, R., S. Druckmann, M. Ottolenghi, and R. Korenstein. 1977. Electric field effects in bacteriorhodopsin. *Biophys. J.* 19:1–5.

Stoeckenius, W., R. H. Lozier, and R. A. Bogomolni. 1979. Bacteriorhodopsin and the purple membrane of halobacteria. *Biochim. Biophys. Acta.* 505:215–278.

Stoylov, S. P., G. Todorov, and A. Zhivkov. 1984. Effect of external electric field on membrane proteins: The bacteriorhodopsin. *Bioelectrochem. Bioenerg.* 12:49–55.

Taneva, S. G., N. Jordanova, and I. B. Petkanchin. 1992. Electro-optical investigation of lipid depleted purple membranes. *Biophys. Chem.* 44: 91–97.

Taneva, S. G., G. Todorov, I. B. Petkanchin, and S. P. Stoylov. 1987. Electrooptic study of the deionized form of bacteriorhodopsin. *Eur. Biophys. J.* 14:415–421.

Tributsch, H., and R. A. Bogomolni. 1994. Bacteriorhodopsin: A molecular photooscillator? *Chem. Phys. Lett.* 227:74–78.

Tsuji, K., and B. Hess. 1986. Electric field induced conformational changes of bacteriorhodopsin in purple membrane films. I. DC field effects. *Eur. J. Biophys.* 13:273–280.

Tsuji, K., and B. Hess. 1990. Electrooptical studies on proton-binding and release of bacteriorhodopsin. *Eur. J. Biophys.* 18:63–69.

Tsuji, K., S. C. Müller, and B. Hess. 1988. Electric field induced conformational changes of bacteriorhodopsin in purple membrane films. II. Alternating field effects. *Eur. J. Biophys.* 15:329–337.

Tsuji, K., and E. Neumann. 1981a. Structural changes in bacteriorhodopsin induced by electric impulses. *Int. J. Biol. Macromol.* 3:231–242.

Tsuji, K., and E. Neumann. 1981b. Electric-field induced pK-changes in bacteriorhodopsin. *FEBS Lett.* 128:265–268.

Tsuji, K., and E. Neumann. 1983. Conformational flexibility of membrane proteins in electric fields. I. Ultraviolet absorbance and light scattering of bacteriorhodopsin in purple membranes. *Biophys. Chem.* 17:153–163.

Unwin, P. N. T., and R. Henderson. 1975. Molecular structure determination by electron microscopy of unstained crystalline specimens. *J. Mol. Biol.* 94:425–440.

Wegener, W. A. 1986. Transient electric birefringence of dilute rigid-body suspensions at low field strengths. *J. Chem. Phys.* 84:5989–6004.

Wegener, W. A., R. M. Dowben, and V. J. Koester. 1979. Time-dependent birefringence, linear dichroism, and optical rotation resulting from rigid body rotational diffusion. *J. Chem. Phys.* 70:622–623.